The Astrophysical Journal, 886:87 (5pp), 2019 December 1 https://doi.org/10.3847/1538-4357/ab4901

Constraining the Equation of State of Neutron Stars through GRB X-Ray Plateaus

Shuang Du[1,2], Enping Zhou[1,3], and Renxin Xu[1]
[1] State Key Laboratory of Nuclear Physics and Technology, School of Physics, Peking University, Beijing 100871, People's Republic of China
dushuang@pku.edu.cn, r.x.xu@pku.edu.cn
[2] Department of Physics and Astronomy, Sun Yat-Sen University, Zhuhai 519082, People's Republic of China
[3] Max Planck Institute for Gravitational Physics (Albert Einstein Institute), Am Muhlenberg 1, Potsdam-Golm, D-14476, Germany
Received 2019 August 4; revised 2019 September 12; accepted 2019 September 23; published 2019 November 22

Abstract

The unknown equation of state (EoS) of neutron stars (NSs) is puzzling because of rich non-perturbative effects of strong interaction there. A method to constrain the EoS using the detected X-ray plateaus of gamma-ray bursts (GRBs) is proposed in this paper. Observations show some GRB X-ray plateaus may be powered by strongly magnetized millisecond NSs. The properties of these NSs should then satisfy: (i) the spin-down luminosity of these NSs should be brighter than the observed luminosity of the X-ray plateaus; and (ii) the total rotational energy of these NSs should be larger than the total energy of the X-ray plateaus. Through the case study of GRB 170714A, the moment of inertia of NSs is constrained as $I > 1.0 \times 10^{45}\left(\frac{P_{\rm cri}}{1\ {\rm ms}}\right)^2\ {\rm g\ cm^2}$, where $P_{\rm cri}$ is the critical rotational period that an NS can achieve. The constraint of the radii of NSs according to GRB 080607 is shown in Table 1.

Unified Astronomy Thesaurus concepts: Neutron stars (1108); Gamma-ray bursts (629); Particle astrophysics (96)

1. Introduction

Determining the equation of state (EoS) of neutron stars (NSs) is very important for the cognition of low-energy strong interaction (Glendenning 1992; Weber 2005; Xu 2018). Common approaches to constrain the EoS are measuring the mass and radius of an NS, or making constraints on the maximum mass of nonrotating NSs. Our knowledge of the EoS of dense matter has been greatly improved by the recent observation of gravitational-wave (GW) radiation from a binary neutron star (BNS) merger (GW170817; Abbott et al. 2017a) and its electromagnetic counterparts (Abbott et al. 2017b; see a recent review Baiotti 2019). The fate of the merger remnant is tightly related to the properties of NS EoSs, and it is with regret that the post-merger remnant of GW170817 is undetermined (Abbott et al. 2019). Although, the total mass of the NS binary $\sim 2.7\,M_\odot$ (Abbott et al. 2017b) is much larger than the measured masses of galactic pulsars, the EoS with a higher upper limit on rest mass as high as $3.0\,M_\odot$ is still not ruled out (e.g., strangeon star; see Yu et al. 2018; Lai et al. 2019; Piro et al. 2019).

On the other hand, the radii of NSs are so small that they have been hard to accurately measure either through the observation of electromagnetic waves or gravitational waves until now. By modeling periodic brightness oscillations of "hotspots" on spinning pulsars, some NSs radii can be constrained (see Özel & Freire 2016 for review). For example, assuming the NS with a mass of $1.4\,M_\odot$, the analysis of PSR J0437-4715 leads to the radius $R(1.4\,M_\odot) \in (6.8\text{–}13.8)\,{\rm km}$ (90% confidence level; Bogdanov et al. 2007). Similarly, an analysis of an NS binary merger, GW170817, whose tidal deformability $\Lambda(1.4\,M_\odot) < 800$, yields $R(1.4\,M_\odot) \in (9.9\text{–}13.6)\,{\rm km}$ (90% confidence level; Annala et al. 2018). Therefore, other observations related to BNS merger remnants are valuable as independent constraints on EoS models.

In this paper, we propose a new approach to constrain the EoS of NSs through the X-ray plateaus of gamma-ray bursts (GRBs). GRBs can be classified into two categories based on duration T_{90}: (Kouveliotou et al. 1993) short GRBs with $T_{90} < 2\,{\rm s}$ (originated from double NS mergers; Abbott et al. 2017b) and long GRBs with $T_{90} > 2\,{\rm s}$ (originated from massive star collapses; MacFadyen & Woosley 1999). Short or long-lived rotationally supported NSs may be born in GRBs (Duncan & Thompson 1992; Usov 1992; Dai & Lu 1998a), which depends on the remnant masses of these catastrophes. In principle, the nascent NSs, both conventional NSs and strange stars, can be strongly magnetized (so-called magnetar) through differential-rotation-induced or convection-induced turbulent dynamo process (Duncan & Thompson 1992; Xu & Busse 2001; Tobias 2019). If the central object of a GRB is a millisecond magnetar, the energy injection (Dai & Lu 1998b; Zhang & Mészáros 2001) by spin-down wind of the magnetar may result in an X-ray plateau followed by a power-law decay with index ~ -2. This theoretical expectation was observed by the *Swift* X-Ray Telescope (XRT; Evans et al. 2009) and further strengthened by a recent observation that the measured light curve of the X-ray transient CDF-S XT2 is consistent with the plateau predicted by the millisecond magnetar born in an NS binary merger (Xue et al. 2019). Additionally, some X-ray plateaus can be followed by a very steep decay (with an index < -3, the so-called "internal plateau;" see, e.g., Troja et al. 2007). This feature can be reasonably explained under the magnetar scenario (see Kumar & Zhang 2015 for review). The spin-down radiation of the supramassive magnetar powers the X-ray internal plateau. The transition from the supramassive magnetar to the black hole through gravitational collapse after losing rotation energy may naturally account for the steep decay.

The luminosities and durations of these X-ray plateaus (case 1: plateau + a decay with index ~ -2; case 2: plateau + a steep decay with index < -3) are closely related to the properties of the central NSs (Du et al. 2016, 2019). So through analyzing the relevant observation data, one may in turn constrain the properties of these NSs, such as the EoS. We describe our method in Section 2. In Section 3, two case studies are shown. In Section 4, the angular distribution of the spin-down wind is discussed. Section 5 is the summary.

2. The Method

The X-ray plateau is powered by the approximately isotropic spin-down wind of the central magnetar (see e.g., Spruit et al. 2001; we discuss the angular distribution of the spin-down flux in Section 4), such that the spin-down luminosity $L_{\rm sd}$ should be larger than the luminosity of the X-ray plateau $L_{\rm X,pla}$, i.e.,

$$L_{\rm sd}=\frac{8\pi^4B_{\rm eff}^2R^6}{3c^3P^4}>L_{\rm X,pla}, \tag{1}$$

where R is the equatorial radius, P is the NS period, $B_{\rm eff}$ is the effective dipole magnetic field strength on the NS surface (perpendicular to the rotation axis of the NS), and c is the speed of light. On the other hand, the initial total rotational energy $E_{\rm k,0}$ of the magnetar should be high enough to power the whole X-ray plateau, so one has (the $=$ is for the case 1, the $>$ is for the case 2)

$$E_{\rm k,0}/L_{\rm sd}\geqslant t_{\rm b}, \tag{2}$$

where

$$E_{\rm k,0}=2\pi^2I/P_0^2, \tag{3}$$

P_0 is the initial period, $t_{\rm b}$ is the break time of the X-ray plateau, and I is the moment of inertia of the magnetar.

According to Equations (1)–(3) one has

$$P_{\rm cri}<P_0<\left(\frac{2\pi^2I}{t_{\rm b}L_{\rm X,pla}}\right)^{1/2}, \tag{4}$$

$$I>\frac{P_{\rm cri}^2}{2\pi^2}\int_0^{t_{\rm b}}L_{\rm X,pla}\,dt, \tag{5}$$

where $P_{\rm cri}$ is the critical period that NSs can achieve.

For a certain EoS, given a magnetar mass $M_{\rm mag}$, one can calculate the theoretical values of the radius $R_{\rm th}$, rotational inertia $I_{\rm th}$, and $P_{\rm cri}$ numerically (see, e.g., Weber & Glendenning 1992). Because $t_{\rm b}$, $L_{\rm X,pla}$ are measurable quantities, the constraint of $I_{\rm th}$ (i.e., Equation (5)) is less model-dependent. Additionally, the masses of the central NSs $M_{\rm mag}$ can be roughly classified as three types:

(i) case 1+short GRB: $2.2\,M_\odot<M_{\rm mag}<\sim M_{\rm TOV}$, where $M_{\rm TOV}$ is the maximum NS mass for a nonrotating NS. The lower limit is inferred form the newest observation that the mass of PSR J0740 + 6620 is $2.17\pm0.11\,M_\odot$ (68% confidence level; Cromartie et al. 2019). More strictly, the lower limit can be taken as the current record $\sim2.0\,M_\odot$ (Antoniadis et al. 2013);

(ii) case 1+long GRB: $M_{\rm mag}\sim1.4\,M_\odot$, as the mass of the individual galactic NS is around $1.4\,M_\odot$ (Özel & Freire 2016);

(iii) case 2: $M_{\rm max}<M_{\rm mag}<1.3M_{\rm max}$, because if $M_{\rm mag}$ is larger than 1.3 times the maximum mass of a rotating NS $M_{\rm max}$, the nascent NS will collapse to a black hole during its dynamical timescale (Baiotti et al. 2008; Hotokezaka et al. 2011). We already know that $M_{\rm max}$ is either greater than $2.7\,M_\odot$ or less than $2.7\,M_\odot$ (Abbott et al. 2017b).

For the magnetars under these three types, I should also be consistent with the mass range.

The constraint of R cannot be as rigorous as I. If magnetars do exist in case 1 and case 2, there is at least one pair of parameters ($B_{\rm eff,max}$, $P_{\rm cri}$) that makes Equation (1) work, i.e.,

$$R>6.9\times10^5\left(\frac{P_{\rm cri}}{1\ {\rm ms}}\right)^{1/3}\left(\frac{B_{\rm eff,max}}{10^{15}\ {\rm Gs}}\right)^{-1/3}\times\left(\frac{L_{\rm X,pla}}{10^{48}\ {\rm erg\ s^{-1}}}\right)^{1/6}{\rm cm}. \tag{6}$$

In principle, according to the dynamo mechanism, $B_{\rm eff}$ has a upper limit (Duncan & Thompson 1992):

$$B_{\rm eff,max}=3\times10^{17}(P/1\ {\rm ms})^{-1}\,{\rm G}. \tag{7}$$

But the observations of soft gamma repeaters (SGRs) and anomalous X-ray pulsars (AXPs) show that almost all the associated magnetars have periods $P_{\rm t}\in(1\text{–}10)$ s, time derivative of period $\dot{P}_{\rm t}\in(10^{-11}\text{–}10^{-10})$ s s^{-1}, and inferred magnetic fields $B_{\rm eff}\in(10^{14}\text{–}10^{15})$ Gs (except for the uncertain magnetic field strength of SGR 1806-20, whose upper limit is perhaps as high as 2.5×10^{15} Gs; see Woods et al. 2007). The existence of the X-ray plateaus shows that the periods of the nascent magnetars are $\sim$1 ms (Rowlinson et al. 2013; Du et al. 2016). If this is also true for the magnetars in SGRs and AXPs, through the assumption that the magnetic moments of these magnetars do not change significantly, the ages of these magnetars are

$$\tau\approx\frac{P_{\rm t}}{2\dot{P}_{\rm t}}\sim10^4\ {\rm yr}. \tag{8}$$

So these magnetars are young NSs, which is consistent with the observation and model of SGRs (e.g., Cline et al. 1982; Katz 2016). Additionally, if the decay of the magnetic torque of a magnetar is consistent with the galactic pulsars for which the decay timescale of the magnetic torque $\tau_{\rm D}\sim(10^6\text{–}10^7)$ yr (Lyne et al. 1975), one finds $\tau\ll\tau_{\rm D}$, such that the assumption of quasi-constant magnetic torque is reasonable. Hereafter, we take the upper limit of $B_{\rm eff}$ as $B_{\rm eff,max}=10^{15}$ Gs and $B_{\rm eff,max}=2.5\times10^{15}$ Gs empirically.

In the above discussion, the gravitational radiation of magnetars is ignored to be conservative. If we were to take the gravitational radiation into consideration, the constraint Equations (5) and (6) would be tighter because the required $E_{\rm k,0}$ would be larger. Actually, whether the spin-down of a example is dominated by gravitational radiation can be inferred from the X-ray afterglow. From conservation of energy, the spin-down of the magnetar is generally read as (Shapiro & Teukolsky 1983)

$$I\Omega\dot{\Omega}=-L_{\rm em}-L_{\rm gw}=-\frac{B_{\rm eff}^2R^6\Omega^4}{6c^3}-\frac{32GI^2\epsilon^2\Omega^6}{5c^5}, \tag{9}$$

where ϵ and $\Omega=2\pi/P$ are the ellipticity and angular velocity of the NS, respectively, and the over dot is the time derivative. The asymptotic solution of Equation (9) can be solved as follows (Lasky & Glampedakis 2016): when the magnetic dipole radiation dominates the spin-down,

$$L_{\rm sd}(t)=L_{\rm sd,0}\left(1+\frac{t}{\tau_{\rm em}}\right)^{-2}, \tag{10}$$

where

$$\tau_{\rm em} = \frac{3c^3 I}{B_{\rm eff}^2 R^6 \Omega_0^2}, \quad (11)$$

and $L_{\rm sd,0}$ and Ω_0 are the luminosity and angular velocity at $t = 0$. When the spin-down is dominated by gravitational radiation

$$L_{\rm sd} = L_{\rm sd,0}\left(1 + \frac{t}{\tau_{\rm gw}}\right)^{-1}, \quad (12)$$

where

$$\tau_{\rm gw} = \left(\frac{5c^5}{128 G I \epsilon^2 \Omega_0^4}\right). \quad (13)$$

Note that the decay of gravitational radiation ($L_{\rm gw} \propto \Omega^6$) is faster than the decay of magnetic dipole radiation ($L_{\rm em} \propto \Omega^4$). Once the spin-down is dominated by the gravitational radiation, initially there will be a moment τ_* at which the spin-down luminosity changes from being gravitational-radiation-dominated to being dominated by magnetic dipole radiation (Zhang & Mészáros 2001; Lasky & Glampedakis 2016), i.e.,

$$\tau_* = \frac{\tau_{\rm em}}{\tau_{\rm gw}}(\tau_{\rm em} - 2\tau_{\rm gw}). \quad (14)$$

So the decay index of the X-ray afterglow will be changed as $\sim 0 \rightarrow \sim -1 \rightarrow \sim -2$ (several candidates can be seen in Yu et al. 2010; the case studies in Section 3 are not in this situation). Additionally, there is another interesting issue. For a given EoS, one roughly has R and I. Through the effect of the gravitational radiation on the slope of X-ray light curves, $\tau_{\rm gw}$ and τ_* are measurable in some cases. Combining Equations (1), (11), (13), and (14), one can estimate ϵ.

3. Case Studies

Until now we have not found a extreme sample that can make a tight limit on I. For example, for GRB 170714A, whose total energy of the X-ray plateau is from 0.3–10 keV (the luminosity of the X-ray plateau is from Hou et al. 2018). Differing from Hou et al. 2018, we assume the two plateaus of GRB 170714A are all powered by spin-down wind:

$$E_{\rm X,pla} = \int_0^{t_{\rm b}} L_{\rm X,pla}\, dt \approx 2.0 \times 10^{52}\ {\rm erg}. \quad (15)$$

Through Equation (5), one has

$$I > 1.0 \times 10^{45}\left(\frac{P_{\rm cri}}{1\ {\rm ms}}\right)^2\ {\rm g\ cm^2}. \quad (16)$$

Almost all the EoSs can match this result. But it is worth emphasizing that the spin-down energy of magnetars will not be completely converted to X-ray emission, and $E_{\rm X,pla} = 2.0 \times 10^{52}$ erg is just the energy in (0.3–10) keV. Considering these two factors, the value of $E_{\rm X,pla}/E_{\rm k,0}$ should be appropriately less than 1. In the future, if detectors can give a wider energy-band observation to GRB X-ray plateaus, the constraint of Equation (16) will be tighter.

A good sample to constrain R is a brighter X-ray plateau, that meets case 1 or case 2. As an example, a magnetar candidate like GRB 080607 is used as a case study. GRB 080607 is a long GRB with $T_{90} = 79$ s,[4] and redshift $z_0 = 3.04$.[5] We fit the X-ray afterglow of GRB 080607 with a smooth broken power law in which the break time of the plateau is $t_{\rm b} \approx 2200$ s, the decay index before the break is $\alpha_1 \approx -0.01$, and the decay index after the break is $\alpha_2 \approx -2.22$ (see Figure 1). The magnetar candidate of GRB 080607 is type (ii), such that the mass of the magnetar may be around $1.4\,M_\odot$. The mean unabsorbed flux of the X-ray plateau in (0.3–10) keV is $F_{\rm lux} = 2.26^{+0.22}_{-0.19} \times 10^{-10}\ {\rm erg\ cm^{-2}\ s^{-1}}$ (Evans et al. 2009). Adopting a Λ CDM model with $H_0 = 70\ {\rm km\ s^{-1}\ Mpc^{-1}}$, $\Omega_{\rm m} = 0.3$ and $\Omega_\Lambda = 0.7$, one has

$$L_{\rm X,pla}(080607) = 4\pi D_{\rm L}^2 F_{\rm lux} > 1.6 \times 10^{49}\ {\rm erg\ s^{-1}}, \quad (17)$$

where $D_{\rm L}$ is the luminosity distance from the source to the Earth. Through Equation (6), the constraint of R is shown in the top half part of Table 1.[6] Considering that different EoSs have different critical periods, we adopt two different values of $P_{\rm cri}$. The constraint by Equation (6) is conservative, as the shorter the period, the weaker the constraint of R. Noting that the newborn magnetar may have a fast decay but intense GW radiation due to some instabilities (e.g., Andersson 1998; Owen et al. 1998; see Ott 2009 for review), and even differential

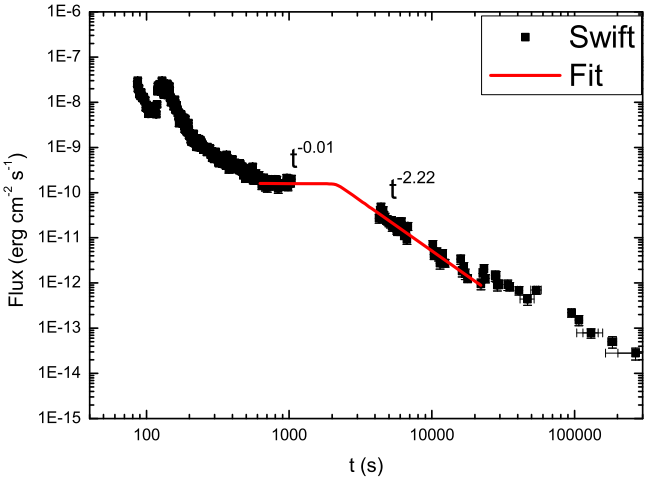

Figure 1. The fitting result of the X-ray afterglow of GRB 080607. The magnetar candidate is clearly type (ii).

Table 1
The Constraint of Equatorial Radius

$B_{\rm eff,max}$ (10^{15} Gs)	$P_{\rm cri}$ (ms)	R (10^5 cm)
1.0	0.5	>8.7
1.0	1.0	>11.0
2.5	0.5	>6.4
2.5	1.0	>8.1
$B_{\rm eff,max}$ (10^{15} Gs)	P_0 (ms)	R (10^5cm)
1.0	1.5	>12.5
2.5	1.5	>9.2
1.0	2.0	>13.8
2.5	2.0	>10.2

[4] Stamatikos et al., GCN 7852, https://gcn.gsfc.nasa.gov/gcn3/7852.gcn3.
[5] Prochaska et al., GCN 7849, https://gcn.gsfc.nasa.gov/gcn3/7849.gcn3.
[6] Note that when the rotation of an NS is near disintegration, i.e., $P \sim P_{\rm cri}$, $B_{\rm eff}$ should be small enough to keep $L_{\rm sd}$ below the jet power.

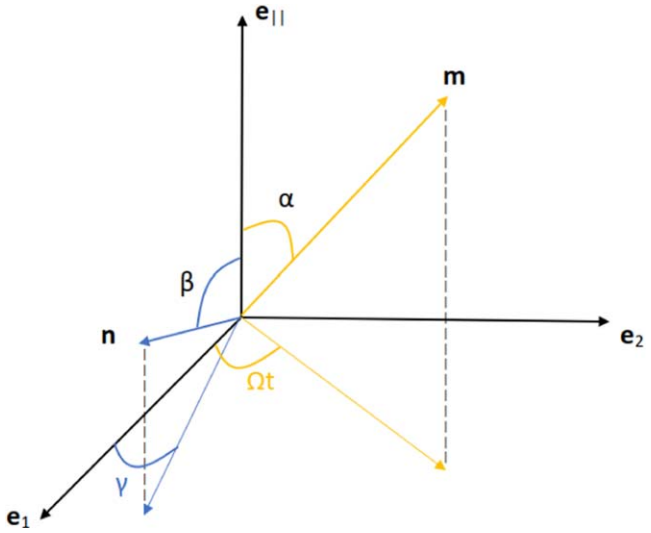

Figure 2. Schematic diagram of the geometric relationship of vectors. $\boldsymbol{e}_{\parallel}$ is a unit vector parallel to the rotation axis, and $\boldsymbol{e}_1$ and $\boldsymbol{e}_2$ are the orthogonal unit vectors perpendicular to the rotational axis.

rotation (Zhou et al. 2019), we also consider a scenario in which the initial period of the magnetar is several times the critical period (see the latter part of Table 1).

4. Angular Distribution

According to electrodynamics (Landau & Lifshitz 1975), the energy flux of the pure magnetic dipole field is

$$\begin{aligned}\boldsymbol{S} &= \frac{1}{4\pi c^3 d^2}|(\ddot{\boldsymbol{m}} \times \boldsymbol{n}) \times \boldsymbol{n}|^2 \boldsymbol{n} \\ &= \frac{1}{4\pi c^3 d^2}|\ddot{\boldsymbol{m}}|^2 \boldsymbol{n} \sin^2\theta, \end{aligned} \tag{18}$$

where $\boldsymbol{n}$ is the unit vector from the source to observer, $\boldsymbol{m}$ is magnetic moment, d is the distance from the source to observer, and θ is the angle between $\boldsymbol{n}$ and $\boldsymbol{m}$. Through the geometry shown in Figure 2, there is

$$\begin{aligned}\cos\theta = (&\cos\beta\cos\alpha + \sin\beta\cos\gamma\sin\alpha\cos\Omega t \\ &+ \sin\beta\sin\gamma\sin\alpha\sin\Omega t). \end{aligned} \tag{19}$$

Then the period average of $\boldsymbol{S}$ is

$$\bar{S} = \frac{1}{4\pi c^3 d^2}|\ddot{\boldsymbol{m}}|^2\left(1 - \cos^2\alpha\cos^2\beta - \frac{1}{2}\sin^2\alpha\sin^2\beta\right), \tag{20}$$

According to Equation (20), there is a critical state $\boldsymbol{n}\|\boldsymbol{e}_{\parallel}$, and $\boldsymbol{n} \perp \boldsymbol{m}$. Therefore, for the NS far away from the Earth, the flux observed on the Earth satisfies

$$F_{\rm lux} \leqslant \bar{S}_{\rm max} = \frac{1}{4\pi c^3 D_{\rm L}^2}|\ddot{\boldsymbol{m}}|^2. \tag{21}$$

Correspondingly, the luminosity of magnetic dipole radiation satisfies

$$L_{\rm em} = \frac{2}{3c^3}|\ddot{\boldsymbol{m}}|^2 = \frac{8\pi}{3}D_{\rm L}^2\bar{S}_{\rm max}, \tag{22}$$

and then there is

$$L_{\rm X,pla} \geqslant \frac{2}{3} \times 4\pi D_{\rm L}^2 F_{\rm lux}. \tag{23}$$

To be more more stringent, the $L_{\rm X,pla}$ in Equation (1) should be divided by $3/2$. However, this angular correction may be offset by the fact that $E_{\rm X,pla}/E_{\rm k,0} < 1$, thus we do not consider it in the above discussion.

5. Summary

In this paper, we aim to propose a new approach to constrain the EoS of NSs. The method to constrain the rotational inertia I is less model-dependent, but the constraint of the radius R is somewhat empirical. Until now, we did not find any perfect samples that could constrain the EoS tightly (similar to the method described in introduction). Two case studies of GRB 170714A and GRB 080607, and the constraints of I and R, are shown in Section 3.

Nevertheless, it should be kept in mind that the radius constraint we enact with this method (i.e., the values shown in Table 1) is on the equatorial radius of a massive rotating neutron star formed either by the collapse of a massive star (in the case of long GRB) or a BNS merger (in the case of short GRB). Therefore, it should not be directly compared with other constraints, such as the GW170817 constraint (i.e., $R(1.4\,M_\odot) \in (9.9\text{–}13.6)$ km), which is on the radius of a nonrotating $1.4\,M_\odot$ NS. However, in the future, those constraints can be combined together if an X-ray plateau observation is achieved together with the GW observation of a BNS merger. In addition to $R(1.4\,M_\odot)$ or $\Lambda(1.4\,M_\odot)$, the GW observation will provide information about the mass and even spin frequency (if a post-merger GW signal could be obtained) of the remnant magnetar. Meanwhile, our method can provide constraints on the rotational inertia and equatorial radius. If our method is correct, any EoS model should satisfy these constraints through GW observation, as well as the constraints imposed by the associated X-ray plateaus at the same time.

To improve the method described in Section 2, one can consider the angular distribution of the spin-down winds of NSs (e.g., Section 4) and the relativistic modification on the rotational energy of NSs (through numerical relativity). In order to produce a better constraint, there are two possible improvements: (a) widening the observational energy band, e.g., 0.1–30 keV or higher, depending on the hard X-ray telescope (e.g., HXMT, Zhang et al. 2014; eXTP, Zhang et al. 2016); and (b) searching for some extreme samples with long-duration and bright X-ray plateaus.

We thank the anonymous referee for helpful comments. We acknowledge the use of the public data from the *Swift* data archives. We thank Fang-Kun Peng for the useful discussion about the estimation of the ellipticities of NSs during the annual meeting "gamma-ray bursts and related frontier physics" in Kunming in January 2018. This work was supported by the National Key R&D Program of China (Grant No. 2017YFA0402602), the National Natural Science Foundation of China (Grant Nos. 11673002, and U1531243), and the Strategic Priority Research Program of Chinese Academy Sciences (Grant No. XDB23010200).

References

Abbott, B. P., Abbott, R., Abbott, T. D., et al. 2017a, PhRvL, 119, 161101
Abbott, B. P., Abbott, R., Abbott, T. D., et al. 2017b, ApJL, 848, L13
Abbott, B. P., Abbott, R., Abbott, T. D., et al. 2019, ApJ, 875, 160
Andersson, N. 1998, ApJ, 502, 708

Annala, E., Gorda, T., Kurkela, A., & Vuorinen, A. 2018, PhRvL, 120, 172703
Antoniadis, J., Freire, P. C. C., Wex, N., et al. 2013, Sci, 340, 448
Baiotti, L. 2019, PrPNP, 109, 103714
Baiotti, L., Giacomazzo, B., & Rezzolla, L. 2008, PhRvD, 78, 084033
Bogdanov, S., Rybicki, G. B., & Grindlay, J. E. 2007, ApJ, 670, 668
Cline, T. L., Desai, U. D., Teegarden, B. J., et al. 1982, ApJL, 255, L45
Cromartie, H. T., Fonseca, E., Ransom, S. M., et al. 2019, NatAs, 3, 439
Dai, Z. G., & Lu, T. 1998a, PhRvL, 81, 4301
Dai, Z. G., & Lu, T. 1998b, A&A, 333, L87
Du, S., Lü, H.-J., Zhong, S.-Q., & Liang, E.-W. 2016, MNRAS, 462, 2990
Du, S., Peng, F.-K., Long, G.-B., & Li, M. 2019, MNRAS, 482, 2973
Duncan, R. C., & Thompson, C. 1992, ApJL, 392, L9
Evans, P. A., Beardmore, A. P., Page, K. L., et al. 2009, MNRAS, 397, 1177
Glendenning, N. K. 1992, PhRvD, 46, 1274
Hotokezaka, K., Kyutoku, K., Okawa, H., Shibata, M., & Kiuchi, K. 2011, PhRvD, 83, 124008
Hou, S.-J., Liu, T., Xu, R.-X., et al. 2018, ApJ, 854, 104
Katz, J. I. 2016, ApJ, 826, 226
Kouveliotou, C., Meegan, C. A., Fishman, G. J., et al. 1993, ApJL, 413, L101
Kumar, P., & Zhang, B. 2015, PhR, 561, 1
Lai, X. Y., Zhou, E. P., & Xu, R. X. 2019, EPJA, 55, 60
Landau, L. D., & Lifshitz, E. M. 1975, The Classical Theory of Fields (Oxford: Pergamon)
Lasky, P. D., & Glampedakis, K. 2016, MNRAS, 458, 1660
Lyne, A. G., Ritchings, R. T., & Smith, F. G. 1975, MNRAS, 171, 579
MacFadyen, A. I., & Woosley, S. E. 1999, ApJ, 524, 262
Ott, C. D. 2009, CQGra, 26, 063001
Owen, B. J., Lindblom, L., Cutler, C., et al. 1998, PhRvD, 58, 084020
Özel, F., & Freire, P. 2016, ARA&A, 54, 401
Piro, L., Troja, E., Zhang, B., et al. 2019, MNRAS, 483, 1912
Rowlinson, A., O'Brien, P. T., Metzger, B. D., Tanvir, N. R., & Levan, A. J. 2013, MNRAS, 430, 1061
Shapiro, S. L., & Teukolsky, S. A. 1983, Black Holes, White Dwarfs, and Neutron Stars: The Physics of Compact Objects (New York: Wiley-Interscience)
Spruit, H. C., Daigne, F., & Drenkhahn, G. 2001, A&A, 369, 694
Tobias, S. 2019, arXiv:1907.03685
Troja, E., Cusumano, G., O'Brien, P. T., et al. 2007, ApJ, 665, 599
Usov, V. V. 1992, Natur, 357, 472
Weber, F. 2005, PrPNP, 54, 193
Weber, F., & Glendenning, N. K. 1992, ApJ, 390, 541
Woods, P. M., Kouveliotou, C., Finger, M. H., et al. 2007, ApJ, 654, 470
Xu, R. 2018, SCPMA, 61, 109531
Xu, R. X., & Busse, F. H. 2001, A&A, 371, 963
Xue, Y. Q., Zheng, X. C., Li, Y., et al. 2019, Natur, 568, 198
Yu, Y.-W., Cheng, K. S., & Cao, X.-F. 2010, ApJ, 715, 477
Yu, Y.-W., Liu, L.-D., & Dai, Z.-G. 2018, ApJ, 861, 114
Zhang, B., & Mészáros, P. 2001, ApJL, 552, L35
Zhang, S., Lu, F. J., Zhang, S. N., & Li, T. P. 2014, SPIE, 9144, 914421
Zhang, S. N., Feroci, M., Santangelo, A., et al. 2016, SCPMA, 62, 029502
Zhou, E., Tsokaros, A., Uryu, K., Xu, R., & Shibata, M. 2019, PhRvD, 100, 043015